JOURNAL OF MATERIALS SCIENCE 14 (1979) 626–632

Static and dynamic fatigue of polycrystalline alumina

J. E. RITTER, Jr
Mechanical Engineering Department, University of Massachusetts, Amherst, Massachusetts 02003, USA

J. N. HUMENIK
I.B.M., Glass and Ceramic Technology Department, East Fishkill, New York 12533, USA

The fatigue failure of polycrystalline alumina was measured in a moist air environment at 30° C as a function of constant applied tensile stress and stressing rate. The good correlation found between the fatigue test data and fracture mechanics theory indicates that fatigue is controlled by the slow crack growth of pre-existing flaws and that static and dynamic fatigue test techniques adequately define the fatigue parameters needed for failure predictions. Comparisons of proof-test predictions with experiment indicate that the proof test can be effective in eliminating weak samples from the population and in assuring against the delayed failure of polycrystalline alumina in a moist environment.

1. Introduction

The use of ceramics in high performance, structural applications is one of the most challenging design areas in today's material science and technology. Unfortunately, ceramic materials exhibit delayed failure (commonly known as static fatigue) and a wide variability in fracture strength that complicate designing for their mechanical reliability. However, a sound, fundamental theory based on fracture mechanics principles [1–4] has recently been developed for making failure predictions for ceramic materials. This theory is based on the reasonable assumption that fatigue failure of ceramics occurs from the stress-dependent growth of pre-existing flaws to dimensions critical for spontaneous crack propagation.

The overall purpose of this study was to determine the applicability of fracture mechanics theory in predicting fatigue failure of polycrystalline alumina under various loading conditions. Although there is substantial evidence that polycrystalline alumina exhibits fatigue failure in moist environments [2, 5–8], there has been no extensive study demonstrating the applicability of fracture mechanics theory in explaining the probability of fatigue failure under various loading conditions and before and after proof testing. To this end, therefore, the fatigue parameters of polycrystalline alumina in moist air were determined by measuring the time to failure as a function of applied stress and by measuring the dependence of fracture strength on stressing rate. These experimental techniques are generally known as static fatigue and dynamic fatigue, respectively [3]. From knowledge of these fatigue parameters, theoretical predictions were made regarding the probability of fatigue failure before and after proof testing and these predictions were then compared to experiment.

2. Experimental procedure and apparatus

All specimens used in this study were alumina bars sintered at 1550° C and containing about 10% of an alkaline earth, aluminosilicate glassy phase (Fig. 1). The average grain size was 4 to 5 μm. The surfaces of the bars were machined flat using a surface grinder* equipped with a horizontal wheel impregnated with 220 grit diamond. After grinding, the tensile surfaces of the bars were abraded by grit blasting with 400 grit alumina and the edges

*Kugel–Muller, Nurnberg, Germany.

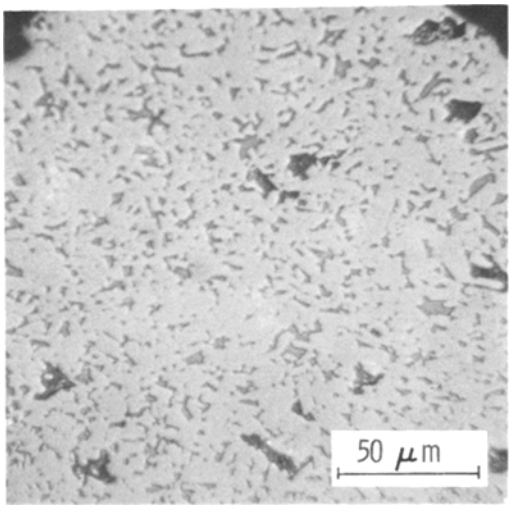

Figure 1 Microstructure of sintered alumina showing distribution of the glassy phase (× 375).

of all the bars were chamferred. The final size of the specimens was nominally 0.172 in. thick, 0.190 in. wide, and 2.5 in. long.

Four-point bending apparatus with an inner span of 0.625 in. and an outer span of 2.125 in. were used for the static and dynamic fatigue tests. Twenty five static fatigue stations with lever arm loading were constructed to permit testing of 25 samples simultaneously. For these static fatigue tests, time to failure under a constant applied stress at six different stress levels was measured for groups of 25 samples each, except in one case where only 13 samples were used. For the dynamic fatigue tests the fracture strength of 25 samples at each of four different stressing rates was measured using a universal testing machine.* Both of the fatigue tests were conducted in a controlled air environment of 30 ± 1° C and 80 ± 5% r.h.

The dynamic fatigue bend test apparatus was also used to measure the fracture strength of 25 samples in liquid nitrogen to determine their strength in an inert environment. In addition, this apparatus was used to proof test a group of samples in ambient air (22° C and 70% RH). These samples were loaded to the proof stress of 45 000 psi† at 2000 psi sec^{-1} and then rapidly unloaded. After proof testing the survivors were divided into three groups of 25 samples each. With one group the inert strength in liquid nitrogen was measured and with the other two groups the failure time at applied stresses of 30 000 and 27 350 psi was determined in the fatigue test environment.

*Instron Corp., Canton, Massachusetts, USA.

† 10^3 psi = 6.89 N mm^{-2}.

3. Results and discussion

3.1. Fatigue failure

Assuming that a single power law relationship exists between the subcritical crack velocity and the stress intensity factor, time-to-failure (t_f) at a constant applied tensile stress can be derived to be [1, 4]:

$$t_f = BS_i^{N-2}\,\sigma_a^{-N}, \qquad (1)$$

where S_i is the fracture strength in an inert environment and B, N are crack growth constants for a given material and environment. Similarly, it can be derived that the fracture strength (S) at a constant stressing rate is [4, 9]:

$$S^{N+1} = B(N+1)\,S_i^{N-2}\,\dot{\sigma}. \qquad (2)$$

The probability of failure (F) for a given t_f and σ_a (or a given S and $\dot{\sigma}$) can be obtained from Equation 1 (or Equation 2) by expressing the inert strength in terms of its failure probability distribution. By so doing, it is assumed that the sample with the shortest fatigue life has the weakest inert strength (largest initial flaw), the median fatigue life has the median inert strength, etc., and that the origin of fracture is the same for both fatigue and inert failures.

Figs. 2 and 3 show the results of the static and dynamic fatigue tests. The static fatigue data were

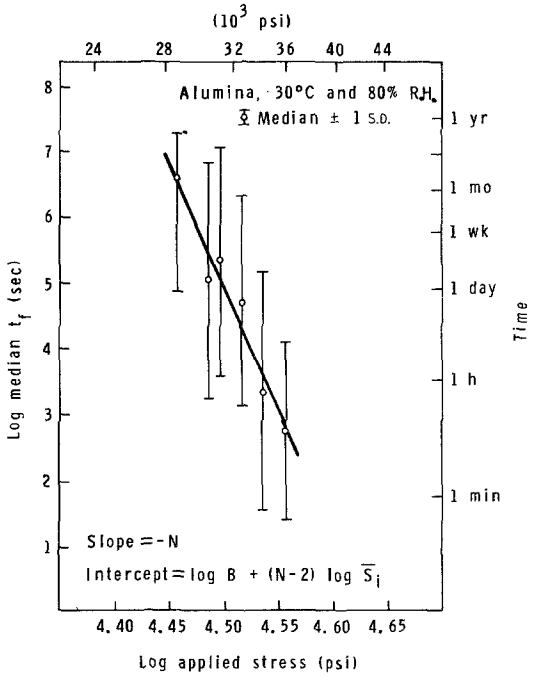

Figure 2 Static fatigue data of polycrystalline alumina in moist air at 30° C.

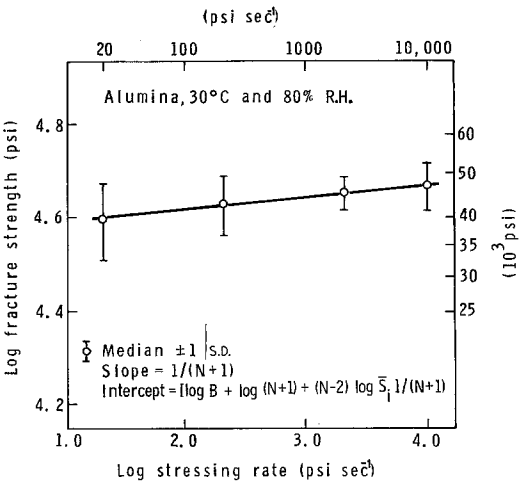

Figure 3 Dynamic fatigue data of polycrystalline alumina in moist air at 30° C.

fitted by least squares analysis to:

$$\log \bar{t}_f = 174.51 - 37.70 \log \sigma_a, \quad (3)$$

where $\bar{t}_f$ = median time to failure at a constant applied tensile stress σ_a and the correlation coefficient to a straight line was 0.97. Similarly, the dynamic fatigue data were fitted to:

$$\log \bar{S} = 4.57 + 2.60 \times 10^{-2} \log \dot{\sigma}, \quad (4)$$

where $\bar{S}$ = median fracture strength at a constant stressing rate of $\dot{\sigma}$ and the correlation coefficient was 0.99. It is evident from these results that a straight line fits the fatigue data well. This indicates that the fatigue data can be adequately represented by Equations 1 and 2 where a simple power law relationship was assumed between subcritical crack velocity and stress intensity factor.

By comparing Equation 3 with Equation 1 the fatigue parameters N and B are given by:

$$37.70 = N$$

$$174.51 = \log B + (N-2) \log \bar{S}_i$$

where $\bar{S}_i$ = median inert strength. Likewise, by comparing Equation 4 with Equation 2, the fatigue parameters in terms of dynamic fatigue data are:

$$2.60 \times 10^{-2} = \frac{1}{N+1}$$

$$4.57 = [\log B + \log (N+1) + (N-2) \log \bar{S}_i]/N + 1. \quad (6)$$

Using these equations with the median inert strength (64 890 psi), the fatigue parameters were determined and are summarized in Table I. Good agreement is obtained between the fatigue parameters as determined from the dynamic and static fatigue tests.

TABLE I Fatigue parameters for polycrystalline alumina in moist air at 30° C

Test technique	N	$\log B$ (psi² sec)
Static fatigue	37.70	2.72
Dynamic fatigue	37.53	3.44

To further compare the fatigue parameters, a lifetime prediction diagram (Fig. 4) was drawn based on Equation 1 and using the fatigue parameters in Table I. Also shown in Fig. 4 are lifetime predictions based on crack velocity data obtained on a similar grade of alumina tested in water [8]. For a lifetime of 1 year, at a stress of 14 500 psi, the predicted (S_i/σ_a) values range from 2.2 to 2.3. Thus, the good agreement obtained between the three test techniques for measuring the crack growth constants indicates that fatigue failure of alumina in moist environments occurs by subcritical crack growth from pre-existing flaws, and that this crack growth can be characterized by crack velocity, static fatigue, or dynamic fatigue experiments.

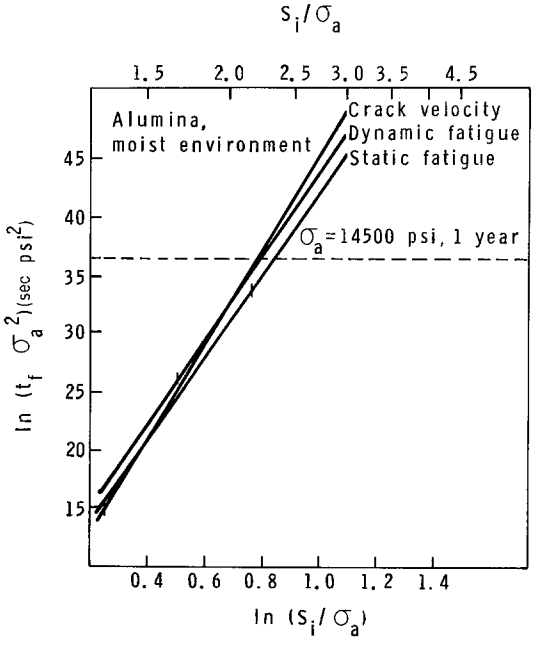

Figure 4 Lifetime prediction diagram comparing crack velocity, dynamic fatigue, and static fatigue data on polycrystalline alumina in a moist environment. The upper limit of the respective experimental data is indicated by the vertical line.

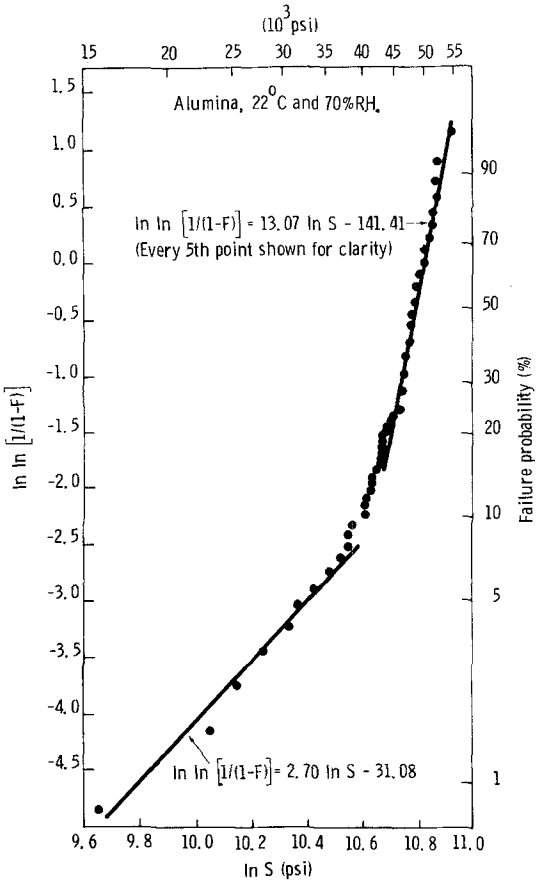

Figure 5 Weibull strength distribution of polycrystalline alumina in ambient air for stressing rate of 2000 psi sec^{-1}.

The applicability of fracture mechanics theory in describing the probability of fatigue failure can be examined by comparing the predicted time-to-failure and strength distributions to those actually measured. The predicted distributions are given by Equations 1 and 2 using the measured fatigue parameters and the inert strength distribution. For the alumina used in this study the inert strength distribution was bimodal; however, the testing of only 25 samples was not enough to clearly define the low strength population. Therefore, to determine more precisely this bimodal strength distribution, especially at the low strength end, the fracture strength of 126 samples was measured in ambient air (22° C, 70% r.h.) at a stressing rate of 2000 psi sec^{-1} and the results are shown in Fig. 5. The appropriate Weibull distributions for the low and high strength populations are:

$$\ln \ln \frac{1}{1-F} = 2.70 \ln S - 31.08,$$

low strength population (7)

$$\ln \ln \frac{1}{1-F} = 13.07 \ln S - 141.41,$$

high strength population (8)

where F is the cumulative failure probability. Based on these strength distributions, the inert strength distributions for the low and high strength populations were determined using Equation 2 to be:

$$\ln \ln \frac{1}{1-F} = 2.49 \ln S_i - 29.53,$$

low strength population (9)

$$\ln \ln \frac{1}{1-F} = 12.05 \ln S_i - 133.94,$$

high strength population (10)

These Weibull inert strength distributions gave a reasonable fit of the inert strength data especially for the high strength population. It should be noted that an attempt was made to determine the origin of the flaw responsible for the low and high strength populations but no success was had in identifying the fracture origin in these samples. However, it is believed that the low strength flaws were a result of gross damage incurred in grinding the samples.

Figs. 6 and 7 compare the experimental data on the probability of fatigue failure with that predicted from Equations 1 and 2 using the bimodal inert strength distribution (Equations 9 and 10). In general, there is good agreement between the predicted and measured distributions; however, it is apparent from the strength distributions that 25 samples are not enough to clearly define the low strength population. It should be noted that the low failure probability distribution was not drawn through the static fatigue data because samples in this low strength population would be the ones recorded as failing on loading. It is believed that this agreement between the predicted and experimental distributions is further evidence that Equations 1 and 2 can be used to adequately represent fatigue failure of alumina in moist environments.

3.2. Proof testing

The purpose of proof testing is to eliminate the weak samples from the population so that the after-proof strength distribution will be stronger than the initial distribution. Evans and Wiederhorn

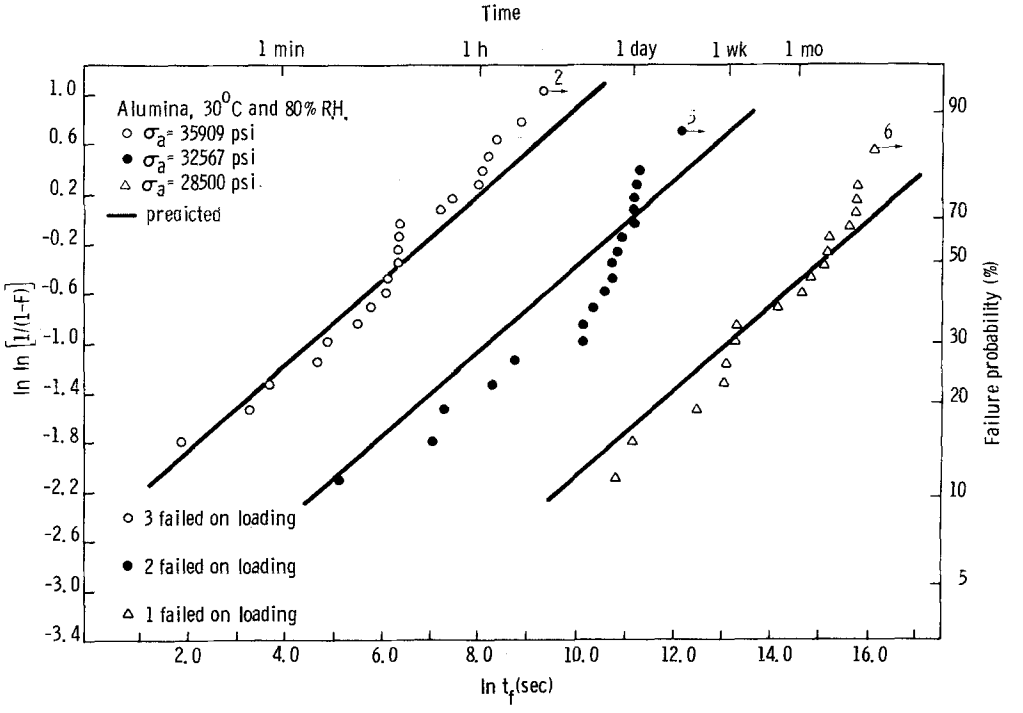

Figure 6 Comparison of the time-to-failure data for polycrystalline alumina in moist air at 30° C to that predicted from Equation 1 coupled with Equations 9 and 10 where the appropriate fatigue parameters were taken to be $N = 37.70$ and $\log B = 2.72$.

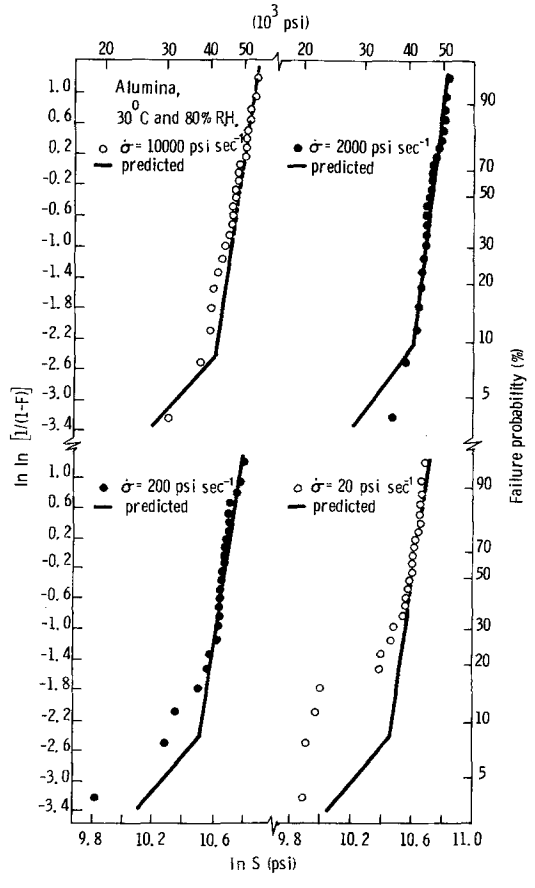

Figure 7 Comparison of the fracture strength data for polycrystalline alumina in moist air at 30° C to that predicted from Equation 2 coupled with Equations 9 and 10 where the appropriate fatigue parameters were taken to be $N = 37.53$ and $\log B = 3.44$.

[1] have shown that the inert strength after proof testing (S_i'), considering crack growth during loading but not unloading is:

$$\left(\frac{S_i'}{S_i}\right)^{N_p-2} = 1 - \left(\frac{\sigma_p^*}{S_i}\right)^{N_p-2}\left[1 - \left(\frac{\sigma_p}{\sigma_p^*}\right)^{N_p-2}\right], \tag{11}$$

where N_p is the fatigue parameter appropriate for the proof test conditions and σ_p^* is the equivalent proof stress for inert conditions, i.e. the proof stress for an inert proof test environment that will result in the same percentage of failures as σ_p does in the actual proof test environment. The failure probability after proof testing (F_a) is related to the initial failure probability by [1]:

$$F_a = \frac{F - F_p}{1 - F_p}, \tag{12}$$

where F_p is the failure probability of the proof test. Thus, for a given N_p, σ_p, and F_p, one can

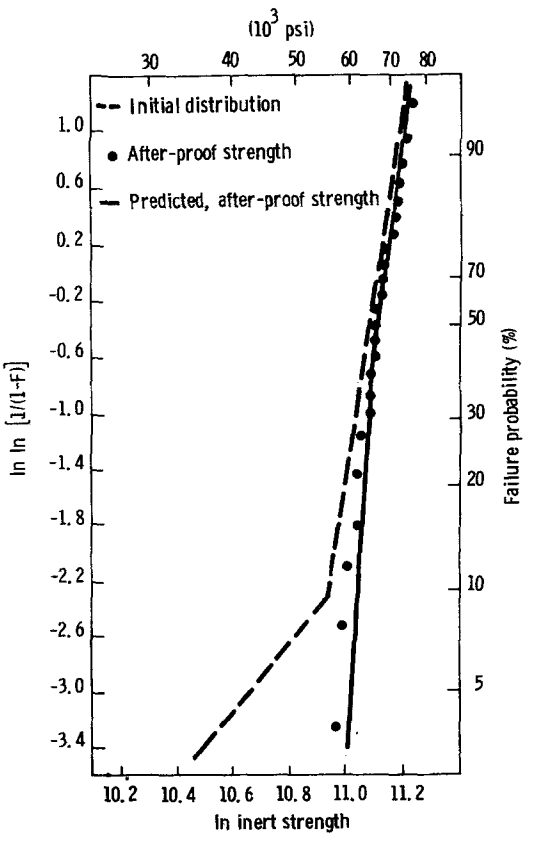

Figure 8 Inert strength distribution of polycrystalline alumina before and after proof testing in air compared to the predicted after-proof strength distribution given by Equation 11 where $\sigma_p = 45\,000$ psi, $N_p = 37.6$, $F_p = 0.30$ and $\sigma_p^* = 61\,800$ psi.

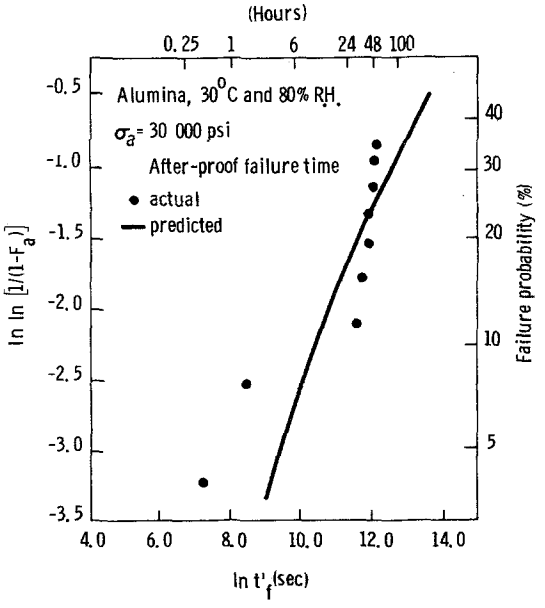

Figure 9 Comparison of the after-proof failure time distribution at $\sigma_a = 30\,000$ psi of polycrystalline alumina in moist air to that predicted from Equation 13 where the fatigue parameters were taken to be $N = 37.70$ and log $B = 2.72$ and $F_p = 0.16$ and $\sigma_p^* = 58\,161$ psi.

calculate the after-proof inert strength distribution using Equations 11 and 12 and the initial inert strength distribution. It is significant to note that inert strength after proof testing is truncated at σ_p and will be greater than the initial inert strength at all levels of failure probability if $m < N_p - 2$. In Fig. 8 the inert strength distribution after proof testing in ambient air is compared to the initial inert strength distribution and to that predicted theoretically from Equation 11. For this proof test, F_p was 0.30 so that the low strength population should be eliminated; thus, from Equation 10 σ_p^* is 61 800 psi. N_p was taken to be equal to that measured in the fatigue tests, 37.6. Good agreement is apparent between theory and experiment and it is evident that proof testing was effective in eliminating the weak specimens from the low strength population.

The lifetime after proof testing (t'_f) is given by an equation similar to Equation 1 except that S_i is replaced by S'_i:

$$t'_f = B\,(S'_i)^{N-2}\,\sigma_a^{-N}. \qquad (13)$$

When S'_i is at its minimum value, i.e. σ_p, Equation 13 then gives the minimum lifetime after proof testing (t_{min}):

$$t_{min} = B\,\sigma_p^{N-2}\,\sigma_a^{-N}. \qquad (14)$$

Equation 14 is most important since it represents the predicted lifetime for no failures in service. Table II compares the experimentally measured minimum time-to-failure after proof testing to that predicted from Equations 13 and 14. Since 25 proof tested samples were tested at each of the applied stresses, the weakest specimen, i.e. the first to fail, had a failure probability of 0.038. It should be noted that in the proof testing of

TABLE II After-proof lifetime predictions compared to experiment for polycrystalline alumina in moist air at 30° C where the appropriate fatigue parameters are taken to be $N = 37.7$ and log $B = 2.72$

Applied stress (psi)	Experimental t'_f ($F = 0.038$) (sec)	Predicted t_{min} (sec)	Predicted t'_f ($F = 0.038$) (sec)
30 000	1.4×10^3	1.83	9.3×10^3
27 350	2.7×10^4	59.76	8.1×10^5

samples for use at the applied stress of 30 000 psi, F_p was 0.16 and for use at the applied stress of 27 350 psi, F_p was 0.30. In both cases the experimental measured failure time was much greater than the predicted t_{min} from Equation 14 and in reasonable agreement with the predicted t_f' for the first failure. Fig. 9 compares the after-proof failure time distribution at 30 000 psi to that predicted from Equation 13. Although only nine samples are included in this distribution, it is seen that the predicted after-proof lifetimes are in reasonable agreement with experiment.

4. Conclusions

(1) The probability of fatigue failure of polycrystalline alumina in moist air correlates well with that predicted from fracture mechanics theory. This indicates that fatigue failure is controlled by slow crack growth of pre-existing flaws and that this subcritical crack growth can be properly characterized by the fatigue parameters as determined from either static fatigue or dynamic fatigue test techniques.

(2) Proof-testing of polycrystalline alumina in ambient air can be effective in eliminating weak samples from the initial distribution. The agreement of after-proof test predictions with experiment indicate that proof testing can be used to insure against the fatigue failure of polycrystalline alumina in a moist environment.

Acknowledgements

The authors are grateful to S. A. Wulf of Brewer Engineering Laboratories who supervised the collecting of the experimental data. One of the authors (J.E.R.) acknowledges the financial support of National Science Foundation grant DMR 77 05647.

References

1. A. G. EVANS and S. M. WIEDERHORN, *Int. J. Fract.* **10** (1974) 379.
2. R. W. DAVIDGE, J. R. McLAREN and G. TAPPIN, *J. Mater. Sci.* 8 (1973) 1699.
3. J. E. RITTER, JUN. and J. A. MEISEL, *J. Amer. Ceram. Soc.* 59 (1976) 478.
4. J. E. RITTER, JUN., "Fracture Mechanics of Ceramics", Vol. 4, edited by R. C. Bradt, D. P. H. Hasselman, and F. F. Lange (Plenum Press, New York and London, 1978) p. 667.
5. A. G. EVANS, *J. Mater. Sci.* 7 (1973) 1137.
6. J. E. BURKE, R. H. DOREMUS, A. M. TURKALO and W. B. HILLIG, "Ceramics in Severe Environments", edited by W. W. Kriegel and H. Palmour III (Plenum Press, New York, 1971) p. 435.
7. J. R. McLAREN and R. W. DAVIDGE, *Proc. Brit. Ceram. Soc.* **25** (1975) 151.
8. G. K. BANSAL, W. H, DUCKWORTH and D. E. NIESZ, *J. Amer. Ceram. Soc.* 59 (1976) 472.
9. A. G. EVANS, *Int. J. Fract.* **10** (1974) 251.

Received 30 December 1977 and accepted 22 May 1978.